Geophys. J. R. astr. Soc. (1984) **79**, 119–133

Synthetic body wave seismograms for three-dimensional laterally varying media

V. Červený and L. Klimeš *Institute of Geophysics, Charles University, Ke Karlovu 3, 121 16 Praha 2, Czechoslovakia*

Accepted, in revised form 1984 January 16

Summary. Two methods of computing body wave synthetic seismograms in three-dimensional laterally varying media are discussed. Both these methods are based on the summation of Gaussian beams. In the first, the initial beam parameters are chosen at the source, in the second at the beam endpoints. Both these variants eliminate the ray method singularities. The expansion of the wavefield into plane waves may be considered as the limiting case of the first approach and the Chapman–Maslov method as the limiting case of the second approach. Computer algorithms are briefly described and numerical examples presented. In the first numerical example, the comparisons of the two approaches, based on summing Gaussian beams, with the reflectivity method indicate that the computed synthetic seismograms are satisfactorily accurate even in the caustic region. The next example suggests that the two methods discussed can be simply and effectively applied to 3-D laterally inhomogeneous structures.

1 Introduction

Recently, the number of seismological problems requiring numerical modelling of seismic wavefields in 3-D laterally varying, layered structures has increased considerably. We know that exact solutions for such models do not exist. Models small in comparison with the prevailing wavelength of the wavefield under investigation can be treated numerically, in principle, by solving the elastodynamic equation directly, e.g. by the method of finite differences or finite elements. However, standard computers can hardly be used for 3-D computations even in small regions.

Many applications involve the evaluation of HF body wave synthetic seismograms in models considerably larger than the prevailing wavelength of body waves being considered. It is then very useful to resort to asymptotic HF methods.

The simplest HF asymptotic method is the ray method. The basic principles of evaluating ray synthetic seismic wavefields have been known for some time (Babich 1956, Karal & Keller 1959, Červený, Molotkov & Pšenčík 1977, for many other references refer to the latter). Although the ray method has several limitations and its accuracy is much poorer in singular regions, computer programs for evaluating ray synthetic seismograms for laterally varying layered structures should prove very useful in various applications.

Several problems occur in applying ray methods to the evaluation of synthetic seismograms in 3-D media. One of the main problems is in two-point ray tracing. Algorithms for reliable determination of all rays of specified elementary wave arriving at the receiver have not been developed yet. Moreover, even the simpler algorithms which do not fully guarantee the determination of all important arrivals are, as a rule, very time-consuming.

A variant of evaluating ray synthetic seismograms, not requiring two-point ray tracing, is described by Červený, Klimeš & Pšenčík (1984). It is based on the paraxial ray approximation. In this method, the displacement vector of the individual elementary wave in the zero-order approximation of the ray method can be evaluated not only on the ray, but also in its close vicinity. The method thus requires only initial-value (Cauchy) ray tracing, covering the region of interest at the Earth's surface with a sufficiently dense system of endpoints of rays. Dynamic ray tracing must then be performed along the rays. Once the endpoints of rays with the dynamic ray tracing results are available, the displacement vector can be evaluated at any point of the region.

However, the paraxial ray approximation does not eliminate the limitations of the ray method, its inaccuracy in singular regions in particular. Some new approaches have been proposed recently which use initial-value rays as a frame, but calculate the amplitudes more accurately even in singular ray regions. This applies to Chapman's application of Maslov theory (Chapman & Drummond 1982), to the method of edge waves of Klem-Musatov (1980), to the Gaussian beam method (see Babich 1968; Kirpichnikova 1971; Červený, Popov & Pšenčík 1982), etc. In another method, called the phase-front method, instead of rays quasi-phase fronts are evaluated and the parabolic wave equations is used to recalculate the wavefield from one phase front to another (see Haines 1983).

Here, we shall describe and use two variants of the Gaussian beam method, and present certain numerical examples of synthetic seismograms for 3-D structures. The method is based on the summation of Gaussian beams, obtained as asymptotic HF one-way solutions of elastodynamic equations highly concentrated to rays. The elastodynamic equation for HF seismic body waves can then be reduced to the parabolic equation. The first variant is based on summing Gaussian beams with the initial parameters of the beams selected at the source and is described in detail in Červený (1983). The second variant is similar but the initial beam parameters are specified at the endpoints of central rays.

Both variants can be used even in the limiting case of infinitely broad Gaussian beams. If plane waves are taken as a special case of infinitely broad Gaussian beams, the expansion of the wavefield into plane waves is obtained in the first variant and the superposition of plane waves at receivers in the second. The latter, in principle, corresponds to the Chapman–Maslov method.

The relevant computer algorithms for both variants are briefly described and numerical results presented. In these examples our synthetic seismograms are first compared with more accurate results (in effect, with the reflectivity method). As this method can only be applied to models with 1-D changes of velocities, the first example deals with such a simple medium. The computations are, of course, performed with the computer programs written for 3-D laterally varying structures. Only after these examples have been dealt with are other examples of synthetic seismograms evaluated by the Gaussian beam method for a 3-D model given.

In the whole paper, we shall consider an isotropic point source of seismic *P*-waves situated close to the upper boundary of the model. The source-time function is considered in the following form:

$$x(t) = \exp\{-[2\pi f_0(t-t_0)/\gamma]^2\} \cos[2\pi f_0(t-t_0) + \nu]. \tag{1}$$

This Gaussian envelope signal (also known as the Gabor signal) is specified by four real-valued parameters: by the prevailing frequency f_0 (Hz), by the t_0 (s), and by two dimensionless parameters, γ and ν. Parameter γ controls the width of the signal. In all the numerical examples, we use $\gamma = 4$, $\nu = 1.57$ and $t_0 = 3/2\, f_0^{-1}$.

We shall assume that receivers are situated at arbitrary points of some region D_0 situated at the upper boundary of the model.

2 Gaussian beam approach

The method based on the summation of Gaussian beams eliminates certain difficulties and limitations of the ray method. It is regular everywhere, including the singular regions of the ray method (the vicinity of caustics, critical regions, the transition regions between the illuminated and shadow zones, etc.). Moreover, it is not as sensitive to the small details of the model as the ray method. Its great advantage is also that the Gaussian beam approach does not require two-point ray tracing but only initial-value ray tracing. Like the ray method, the Gaussian beam method is asymptotic and valid for high frequencies. It is therefore convenient for constructing synthetic body wave seismograms, particularly if the source-time function represents an HF signal. Červený (1983) explained the evaluation of synthetic body wave seismograms using the Gaussian beam method in detail and therefore the description of the method given here will only be very brief.

In very much the same way as in the ray method, the complete wavefield generated by a point source is composed of wavefields corresponding to the individual elementary waves. In the following, only the evaluation of one elementary wave will be described.

In the Gaussian beam method, the wavefield corresponding to one elementary wave is obtained as a superposition of Gaussian beams concentrated close to rays of this elementary wave. Before the method is applied, a 3-D ray diagram must be evaluated. The individual rays are calculated by initial-value ray tracing starting from the point source, as in the paraxial ray method. Assume that the seismic wavefield is to be evaluated in region D_0 at the Earth's surface. The endpoints of the calculated rays must then cover not only region D_0, but also some vicinity of this region. The reason for this is that a Gaussian beam concentrated at a particular ray affects not only the wavefield at the endpoint of the ray, but also the wavefield in some finite neighbourhood of the endpoint.

Let us now select one ray, mark it Ω and evaluate the Gaussian beam concentrated close to it. The procedure of calculating Gaussian beams concentrated close to any ray in a 3-D laterally inhomogeneous smooth medium (without interfaces) is described in detail in Červený & Pšenčík (1983). Here, only several general facts and terms will be mentioned to enable the reader to understand the numerical examples presented in the next section.

As in the paraxial ray method (see Červený *et al.* 1984), it is necessary to evaluate the vector basis of the ray-centred coordinate system and to perform dynamic ray tracing along each ray. The purpose of the dynamic ray tracing is to evaluate the auxiliary matrices $\mathbf{Q}(s)$ and $\mathbf{P}(s)$, which play an important role in the determination of both the paraxial ray approximation and the Gaussian beams. In the Gaussian beam approach, however, the matrices $\mathbf{Q}(s)$ and $\mathbf{P}(s)$ are complex-valued, whereas they are real-valued in the paraxial ray method. An important role is played by the complex-valued matrix $\mathbf{M}(s) = \mathbf{P}(s)\,\mathbf{Q}^{-1}(s)$, known as the complex-valued matrix of the second derivatives of the travel-time field, or by matrix $\mathbf{K} = v\mathbf{M}$, known as the complex curvature matrix. The physical meaning of these matrices is the following: Matrix $\mathrm{Re}\,\mathbf{K}$ is the curvature matrix of the Gaussian beam wavefront, matrix $\mathrm{Im}\,\mathbf{K}$ (or $\mathrm{Im}\,\mathbf{M}$) controls the amplitude profile of the Gaussian beam in the

plane orthogonal to the ray Ω. Note that the amplitude profile along any straight line perpendicular to the ray Ω is bell-shaped.

A very important role in the evaluation of synthetic seismic wavefields by the Gaussian beam approach is played by the selection of initial conditions for the dynamic ray tracing system (initial parameters of Gaussian beams). We can choose the initial conditions for the dynamic ray tracing system at any point $s = s_0$ of the ray in a number of ways, for example,

$$\mathbf{Q}(s_0) = \mathbf{I}, \qquad \mathbf{P}(s_0) = \mathbf{M}(s_0), \tag{2}$$

where $\mathbf{I}$ is a unit matrix and $\mathbf{M}(s_0)$ is the initial complex-valued matrix of the second derivatives of the travel-time field. Matrix $\mathrm{Im}\,\mathbf{M}(s_0)$ must be positive definite to guarantee that the Gaussian beam is concentrated to the central ray Ω. The point $s = s_0$ usually corresponds to the source but may also correspond to some other point on the central ray Ω of the Gaussian beam, e.g. to the endpoint of the ray Ω at the Earth's surface. It is simplest to adopt a diagonal matrix with equal eigenvalues for $\mathbf{M}(s_0)$, for example,

$$\mathbf{M}(s_0) = \left[v^{-1}(s_0)\, K_0(s_0) + \frac{i}{\pi L_0^2(s_0)}\right] \mathbf{I}, \tag{3}$$

where $v(s_0)$ is the velocity at $s = s_0$, and $K_0(s_0)$ and $L_0(s_0)$ are real-valued constants. This case involves a circular (stigmatic) Gaussian beam which has the same properties along any straight line perpendicular to the ray at $s = s_0$. The constants $K_0(s_0)$ and $L_0(s_0)$ determine the curvature of the wavefront of the beam and the beam half-width for the frequency of 1 Hz. For $\mathrm{Im}\,\mathbf{M}(s_0) = 0$, i.e. for $L_0(s_0) = \infty$, the expressions for the Gaussian beams transform to expressions for the paraxial ray approximation. In this sense, the paraxial ray approximation may be considered a limiting case of Gaussian beams.

The final wavefield corresponding to the elementary wave under consideration is obtained by the summation of Gaussian beams with the endpoints of their central rays in some vicinity of the receiver. Remote Gaussian beams need not be considered, their contribution to the final results being small. Details of deriving various forms of these expansion formulae are given and discussed by Klimeš (1984).

Note that the expansion formulae are very flexible because the initial parameters of the Gaussian beams can be chosen at different points and in different ways. It is only necessary to determine the complex-valued normalization factors of the beams correctly for each expansion formula. The two basic possibilities are to choose the initial parameters at the source and at the endpoints of rays. Moreover, the initial width of the Gaussian beams in the expansion formulae may be chosen in different ways, including infinitely broad Gaussian beams. The latter corresponds to the superposition of paraxial ray approximations. Even the paraxial ray approximation offers various possibilities, because the curvature of the wavefront may be chosen in different ways, including the plane-wave approximation. In this sense, the Gaussian beam method includes even the expansion of the point-source wavefield into plane waves and the summation of plane waves at receivers as limiting cases. The latter is close to the Chapman–Maslov method of the second order (Chapman & Drummond 1982). The application of finite-width beams may also be interpreted as the application of Gaussian integration windows in the expansion of the wavefield into plane waves, or in the Chapman–Maslov method.

The method of Gaussian beams may be used both in the frequency and time domains. Several approaches to time-domain computations, based on the Gaussian beam approach, have been derived by Červený (1983). We shall not discuss these approaches here but refer the reader to the reference given above. To evaluate synthetic seismograms, we shall use Gaussian envelope packets. If the source-time function is given by (1), we can evaluate the

wave packets approximately analytically. The final wave packets, called Gaussian packets (or Gaussian envelope packets) have a Gaussian envelope both in time and space. Under the envelope, they of course oscillate. They propagate along the rays and are firmly tied to them. We then obtain the final wavefield, corresponding to the elementary wave being considered, as a superposition of Gaussian packets which propagate along the rays situated in the vicinity of the receiver. Again, Gaussian packets propagating along remote rays need not be considered.

In the following, we shall only speak of summing Gaussian beams for simplicity, although we shall actually be working with Gaussian packets.

3 Numerical examples

In this section, we shall present several examples of body wave synthetic seismograms, computed using the methods discussed above. In the first series of computations in Section 3.1, we shall investigate the accuracy of the individual methods by comparing their results with exact computations. In Section 3.2, we shall present and briefly discuss some results of computations for a 3-D structure with a caustic.

3.1 COMPARISON OF VARIOUS METHODS

To appreciate the accuracy of the various methods, it is possible to compare their results with exact computations or with computations of a high accuracy. Our results will be compared with those obtained using the reflectivity method of Fuchs & Müller (1971). However, this method cannot be used in general 3-D models and therefore the comparisons will be made for a vertically inhomogeneous model for which it can be used. It should be emphasized, however, that all our computations are made with programs which can be used to evaluate synthetic seismograms in very general 3-D layered structures.

Figure 1. Vertically inhomogeneous model used for computing synthetic seismograms.

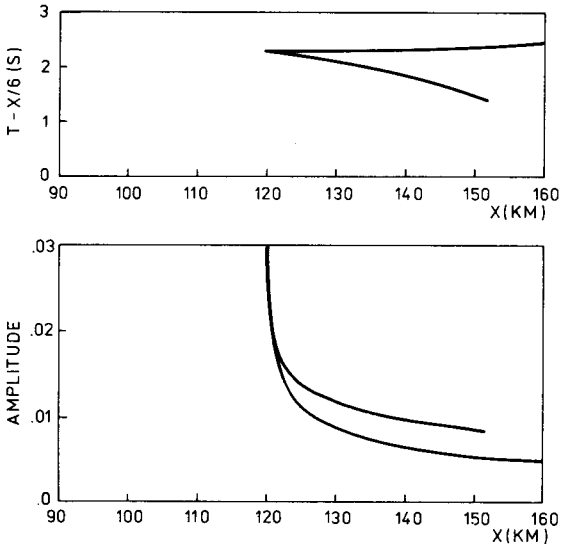

Figure 2. Reduced travel time of the *P*-refracted wave and corresponding ray amplitude–distance curve for the model shown in Fig. 1. The reduced velocity is 6 km s^{-1}. The caustic is formed at $x = 120$ km.

The vertically inhomogeneous model, used for computation, consists of three layers separated by second-order interfaces (Fig. 1). The *P*-velocity in the top layer is constant, 5.6 km s^{-1}. In the second (transition) layer, the *P*-velocity increase linearly from 5.6 km s^{-1} at a depth of 15 km to 8 km s^{-1} at a depth of 40.7 km. The bottom layer (half-space) is again homogeneous with a *P*-velocity of 8 km s^{-1}. The *S*-velocity β and the density ρ are obtained from the *P*-velocity α using the relations $\beta = \alpha/\sqrt{3}$, $\rho = 0.252 + 0.379\alpha$. Note that the same model was used to evaluate the time-harmonic wavefield in the vicinity of the caustic using the 2-D Gaussian beam method in Červený *et al.* (1982).

The point source of *P*-waves is situated close to the Earth's surface which is assumed to be a plane situated at a depth of 0 km. Waves reflected from the Earth's surface are not considered (as in the reflectivity method) and the wavefield corresponds to the refracted wave. The wavefield will be evaluated along a straight line profile containing the source, the profile being positioned along the x-axis. The source-time function is given by (1), with the prevailing frequency f_0 either 2 or 4 Hz in the separate figures.

As the ray diagram for the refracted wave in this model was presented in Červený *et al.* (1982), it will not be shown here. In the above reference it was shown that the refracted wave is formed by two branches with a caustic point at $x = 120$ km. The reduced travel-time curves and the ray amplitude–distance curves of these two branches are depicted in Fig. 2. The branch with smaller travel times corresponds to rays which penetrate deeper into the transition zone. The boundary ray, which touches the bottom of the transition layer at a depth of 40.7 km, arrives at the Earth's surface at an epicentral distance of 151.8 km. For the lower branch of the refracted wave, therefore, a geometrical shadow zone is formed for $x > 151.8$ km.

In the following, we shall compare the synthetic seismograms for the discussed model computed along a profile from $x = 95$ to 155 km. We shall compare the results obtained using five methods:

(a) the reflectivity method;

(b) the Gaussian beam approach with the initial beam parameters specified at the source;

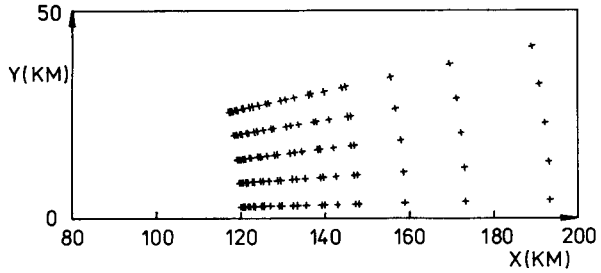

Figure 3. Endpoints of rays used for computing synthetic seismograms by means of the Gaussian beam approach with initial parameters chosen at the source. Due to symmetry the rays were only shot to one side of the profile.

(c) the Gaussian beam approach with the initial beam parameters specified at the endpoints of rays;

(d) the method based on the summation of the paraxial ray approximations with plane wavefronts at the endpoints of rays (close to the Chapman–Maslov method of the second order);

(e) the ray method (the approach based on the paraxial ray approximation).

In the reflectivity method, the transition layer was simulated by a thin-layered medium with layers 1.0714 km thick. To be quite sure, the synthetic seismograms were recalculated with twice the number of layers (thickness 0.5357), but the results showed no changes within 3–4 decimal places.

In the next methods it is first necessary to shoot the rays to some region at the surface, containing the profile. Fig. 3 shows the endpoints of rays used for the computation under the Gaussian beam approach, both for the initial parameters specified at the source and at the endpoints of rays. Due to the symmetry of the model, the rays were shot only to one side from the profile and the results were multiplied by two. The total number of endpoints of rays was 130. In the method based on the summation of paraxial ray approximations with plane wavefronts at endpoints of rays, a larger region and considerably larger ray density had to be considered. In this case, the total number of endpoints of rays was 884, i.e. about seven times larger than in the Gaussian beam method. Even with this large number of rays, the synthetic seismograms obtained for $f_0 = 4$ Hz are not quite stable. In the last method, based on the paraxial ray approximation, rays were only along the profile.

Synthetic seismograms for the vertical displacement vector components of the *P* refracted wave in the model being considered, computed using different methods, are shown for the prevailing frequency of 2 Hz in Fig. 4, and for the prevailing frequency of 4 Hz in Fig. 5. The synthetic seismograms computed by means of the Gaussian beam method with the initial parameters specified at the endpoints of rays are not presented in Figs 4 and 5, as they are very similar to those obtained by means of Gaussian beams with initial parameters specified at the source. A more detailed discussion of these seismograms will be given later. see Fig. 8.

In the synthetic seismograms, computed by means of the *reflectivity method* (Figs 4a and 5a), we can see the well-known behaviour of the wavefield in the vicinity of the caustic. The wavefield does not vanish even in the geometrical shadow in front of the caustic. At the very caustic ($x = 120$ km) the amplitudes increase smoothly. Maximum amplitudes are reached at some distance beyond the caustic, at $x = 120$–130 km. For $f_0 = 4$ Hz, the maximum amplitudes are closer to the caustic. At larger epicentral distances, the refracted wave divides into two branches and the amplitudes decrease along both branches slowly.

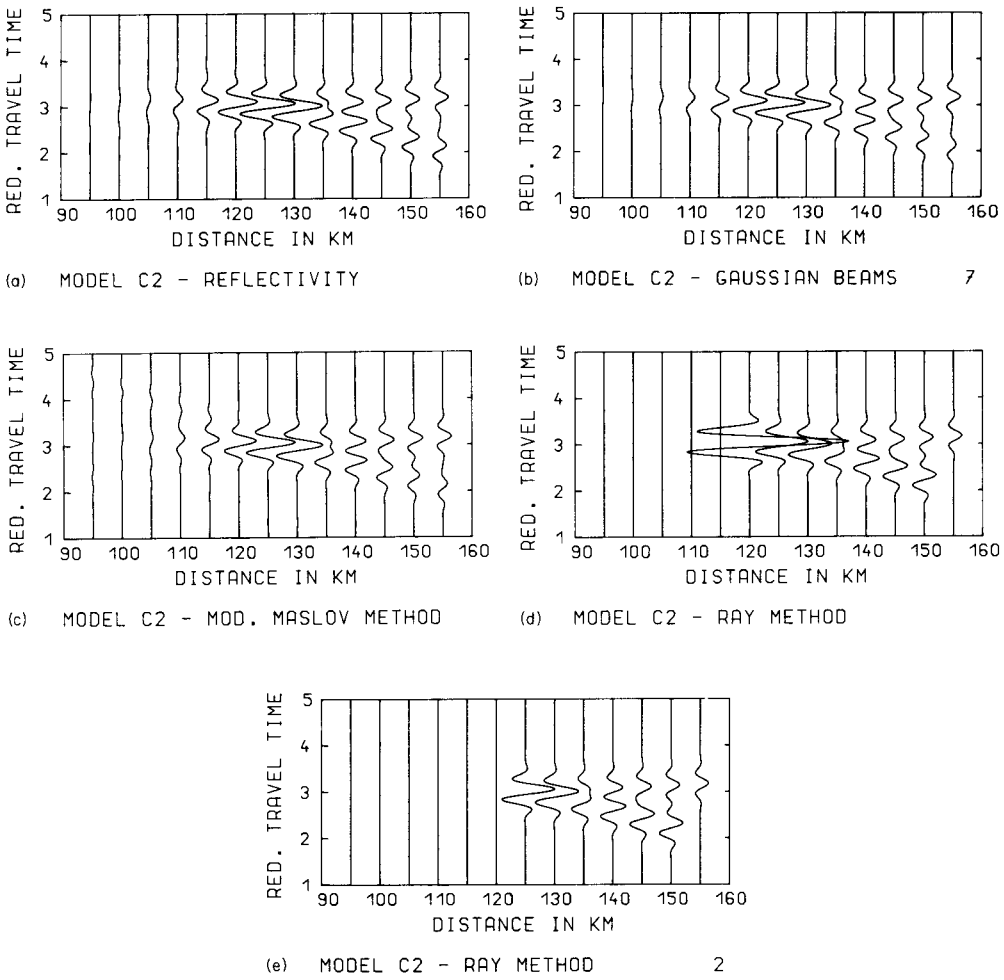

Figure 4. Synthetic seismograms of the vertical displacement vector component of the *P*-refracted wave in the model shown in Fig. 1. The travel-time axes are reduced, the reduction velocity is 6 km s^{-1}. Prevailing frequency 2 Hz. The synthetic seismograms in the individual figures were computed using the following methods: (a) reflectivity method; (b) Gaussian beam method with initial parameters of beams specified at the source. The Gaussian beams are stigmatic (circular) at the source with $L_0 = 16$ km, $K_0 = 0$ km^{-1}; (c) method based on the summation of the paraxial ray approximations with plane wavefronts at the endpoints of rays (a simple version of the Chapman–Maslov method of the second order); (d) ray synthetic seismograms, approach based on the paraxial ray approximation; (e) the same as in (d) but with the anomalous trace $x = 120$ km being excluded.

The wavelets corresponding to both these branches do not have the same form, but there is an obvious phase shift of $\frac{1}{2}\pi$ along one branch.

It is interesting to observe that the wavefield is frequency-dependent in the whole range of epicentral distances being considered by comparing Figs 4(a) and 5(a). The frequency-dependent effects in the vicinity of the caustic were discussed above. The first branch of the refracted wave is frequency-dependent even at larger epicentral distances ($x = 150$–155 km) as a geometrical shadow is formed beyond $x = 151.8$ km due to the bottom of the transition zone. This effect will be discussed in greater detail later. Even in the later branch, however, the amplitudes for $f_0 = 4$ Hz are about 8 per cent higher than those for $f_0 = 2$ Hz at epicentral

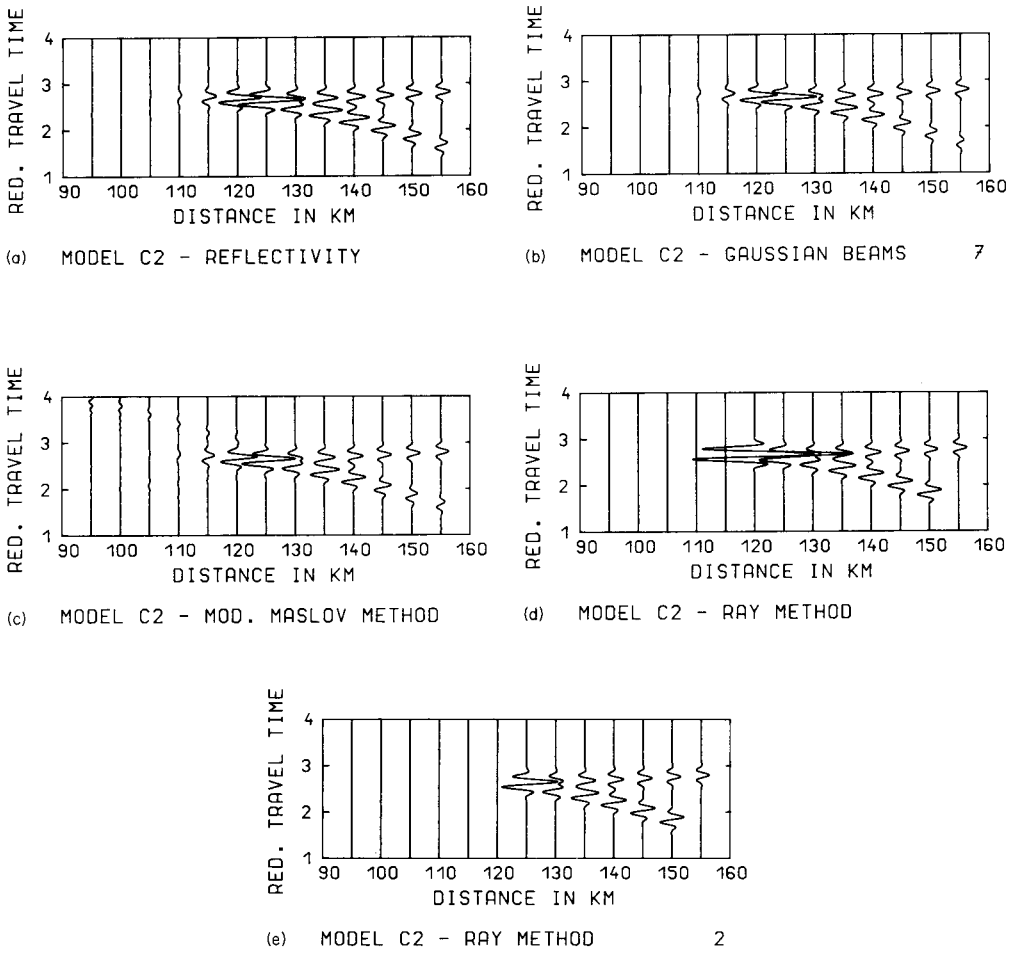

Figure 5. The same as in Fig. 4 but for prevailing frequency of 4 Hz.

distances $x = 150-155$ km. This increase in amplitudes is probably due to the reflections from the discontinuity of the velocity gradient at a depth of 15 km.

The synthetic seismograms produced by the *Gaussian beam approach with the initial parameters specified at the source* (see Figs 4b and 5b) are very similar to those obtained by means of the reflectivity method. The general behaviour of the wavefields computed by means of the reflectivity method and Gaussian beam method is practically the same. The quantitative comparison of the maximum amplitudes in the individual traces, computed using the reflectivity and Gaussian beam method, shows that the amplitudes do not differ by more than 11 per cent in the caustic region. At the epicentral distance of 155 km, the differences are less than 5 per cent.

Results very similar to those obtained with the Gaussian beams were produced by the *summation of the paraxial ray approximations with the plane wavefronts at the endpoints of rays* (Figs 4c and 5c). This method is a simple form of the Chapman–Maslov method (from the computational point of view). For the prevailing frequency of 2 Hz, the amplitudes are again slightly lower than those obtained by the reflectivity method, they rather resemble the results obtained with Gaussian beams, see Fig. 4(b). The differences are somewhat larger for the frequency of 4 Hz, amounting to about 15 per cent in the caustic region.

The larger differences for higher frequencies, however, may also be due to numerical errors in summing rapidly oscillating functions (e.g. due to the insufficient density of rays). This difficulty can simply be overcome by using Gaussian beams with finite widths instead of plane waves at the receivers, see Fig. 8.

Several weak fictitious waves with straight travel-time curves can clearly be seen in Figs 4(c) and 5(c). The waves are distinct especially in the shadow zone in front of the caustic. The strongest of these waves is that with an apparent velocity of about 8 km s^{-1}. The wave is caused by the lower boundary of the integration window over the ray parameter ϕ (initial inclination of the ray). Such fictitious waves are well known from reflectivity seismograms where the integration window over angles of incidence is artificially introduced to make the computations faster. Here, however, the lower boundary of the window corresponds to the bottom of the transition zone at a depth of 40.7 km. No rays with endpoints at the Earth's surface penetrate lower, under the transition zone.

Let us now discuss the *ray synthetic seismograms* (Figs 4d and 5d). It is well known that the ray computations produce a shadow zone in front of caustics ($x < 120$ km). In the vicinity of a caustic, the amplitude is very high and unstable. Beyond the caustic, the wave separates into two branches and the amplitudes of both branches decrease with increasing epicentral distance. The high amplitude at $x = 120$ km is not of great practical value as it corresponds to the singular ray region. It may prove better to eliminate the extremely high amplitudes connected with caustics from the computations, either automatically or manually (see Figs 4e and 5e). In other cases, it may prove valuable to know the exact position of the caustic, in which case it is convenient to retain the high amplitudes in the synthetic seismograms.

Amplitudes of traces for $x \geq 125$ km are close to those obtained with the Gaussian beam method. The maximum differences with respect to the reflectivity method do not exceed 15 per cent. Also the phase shift of $\frac{1}{2}\pi$ can clearly be seen in the ray synthetic seismograms.

In the first branch, the refracted wave is missing at $x \geq 155$ km, see Figs 4(d, e) and 5(d, e). A geometrical shadow zone for this branch of the refracted wave is formed at $x > 151.8$ km due to the bottom of the transition zone. The Gaussian beam synthetic seismograms yield qualitatively correct amplitudes even at $x = 155$ km as can clearly be seen by comparing Figs 4(a) and 4(b) (or 5a and 5b). Other computations (not presented here), however, suggest that the decrease of the amplitudes from the illuminated region to the shadow zone, as obtained at distances $x > 150$ km by means of the Gaussian beam method, is faster than that obtained with the reflectivity method.

The Gaussian packet approach may be influenced by the initial Gaussian beam parameters, i.e. by the choice of quantities K_0 and L_0 (see equation 3). In the above computations quantity K_0 was taken to be equal to 0. Quantity L_0 was taken close to that used by Červený *et al.* (1982) for 2-D time-harmonic Gaussian beams.

To demonstrate the sensitivity of synthetic seismograms to the initial parameters specified at the source, some additional computations were performed with different K_0 and L_0. Figs 6 and 7 show several synthetic sections for the model being considered, computed with different K_0 and L_0 for frequencies of 2 and 4 Hz. As can be seen, the differences between the various computations are small for the chosen range of K_0 and L_0.

In Fig. 8, three synthetic seismogram sections computed by the Gaussian beam approach with the initial parameters of Gaussian beams *specified at the endpoints of rays* are presented. In all the three cases, the plane wavefronts at the endpoints of ray are considered ($K_0 = 0$ km^{-1}), but the Gaussian window is applied (L_0 finite). This considerably increases the effectiveness of computations in comparison with those performed by means of a paraxial approximation summation, shown in Fig. 4(c). Even more, the results are more stable and

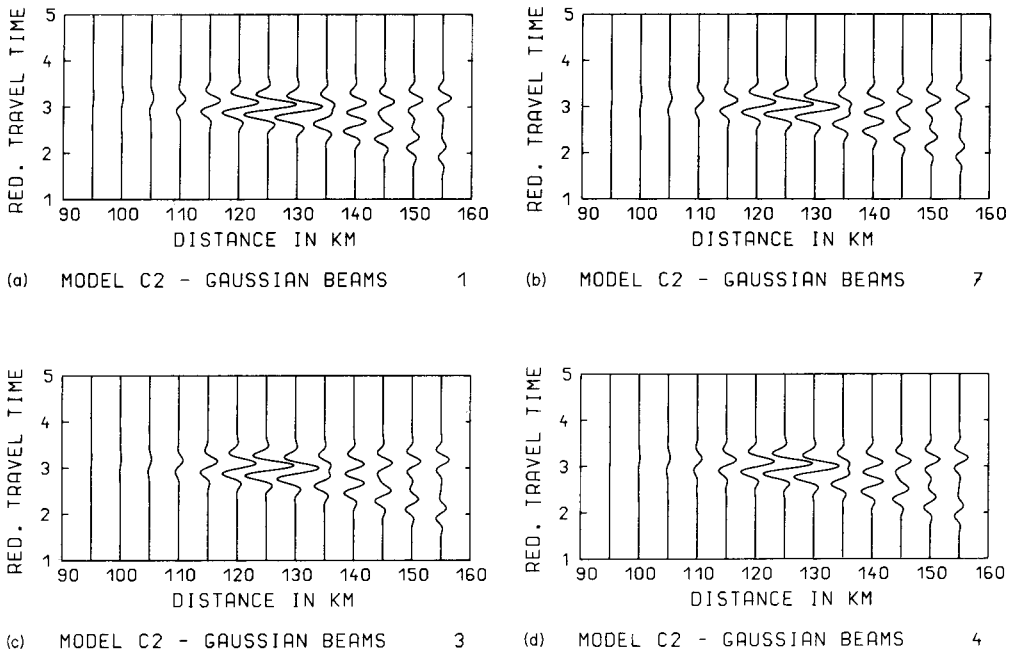

Figure 6. Synthetic seismograms of the vertical displacement vector component of the *P*-refracted wave in the model shown in Fig. 1. All seismograms were computed using the Gaussian beam approach with parameters of the beams specified at the source. Reduction velocity 6 km s^{-1}, prevailing frequency 2 Hz. The Gaussian beams are stigmatic at the source in all cases; parameters L_0 and K_0 are specified as follows: (a) $L_0 = 16$ km, $K_0 = 0.0075$ km^{-1}; (b) $L_0 = 16$ km, $K_0 = 0$ km^{-1}; (c) $L_0 = 16$ km, $K_0 = -0.0075$ km^{-1}; (d) $L_0 = 22.6$ km, $K_0 = 0$ km.

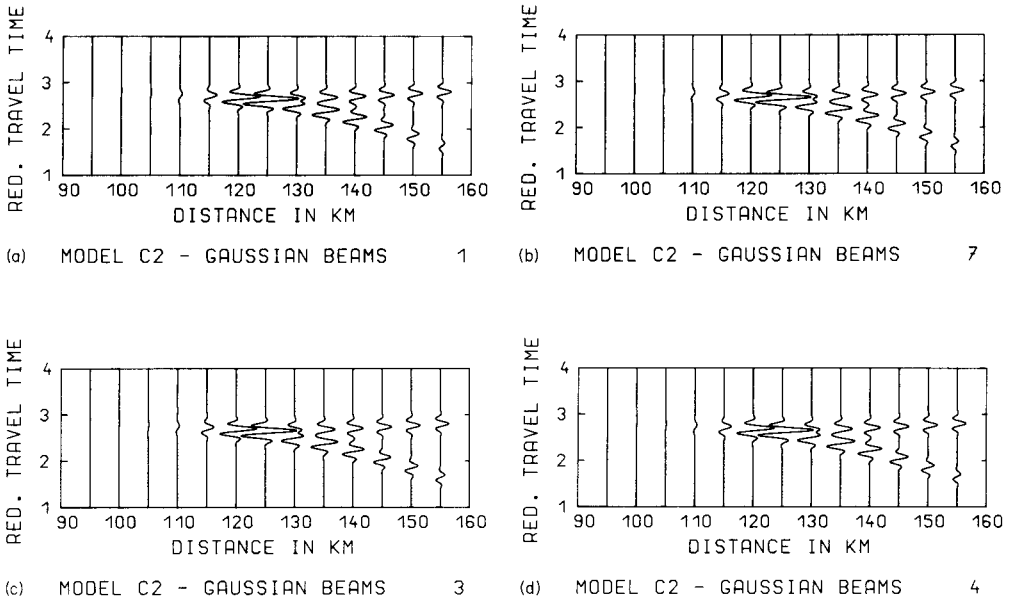

Figure 7. The same as in Fig. 6 but for the prevailing frequency of 4 Hz.

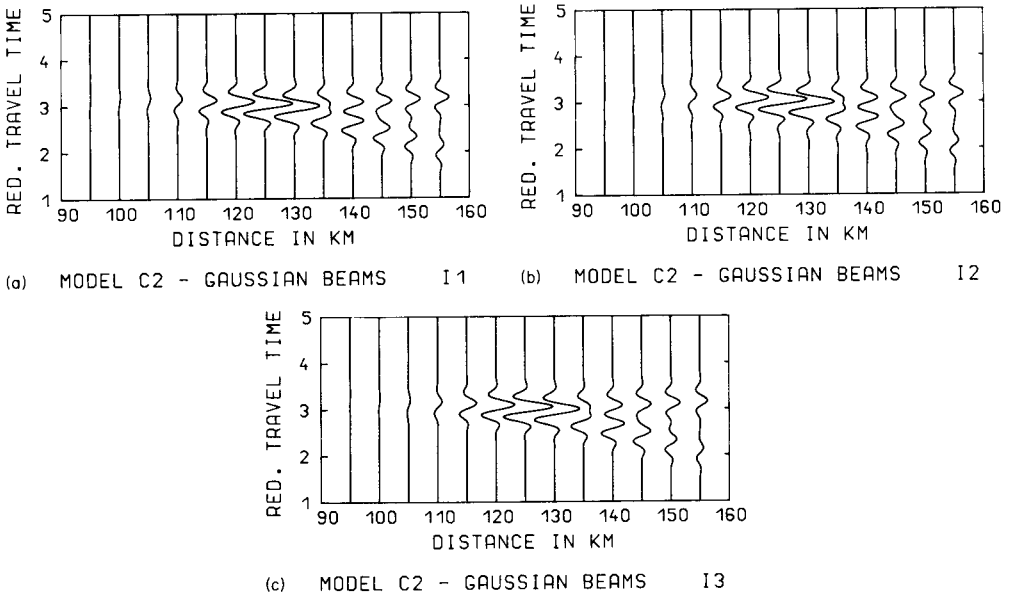

Figure 8. Synthetic seismograms of the vertical displacement vector component of the *P*-refracted wave in the model shown in Fig. 1. The synthetic seismograms were computed using the Gaussian beam approach with parameters specified at the endpoints of rays. Reduction velocity 6 km s^{-1}, prevailing frequency 2 Hz. The initial parameters of Gaussian beams are specified as follows: (a) The beams are stigmatic at the endpoints of rays, with $L_0 = 10$ km, $K_0 = 0$ km^{-1}. (b) The beams are stigmatic at the endpoints of rays, with $L_0 = 14$ km, $K_0 = 0$ km. (c) The beams are elliptical at the endpoints of rays, with $K_0 = 0$ km^{-1} and with a circular spot at the Earth's surface. The circular spot is characterized by $L_0 = 10$ km.

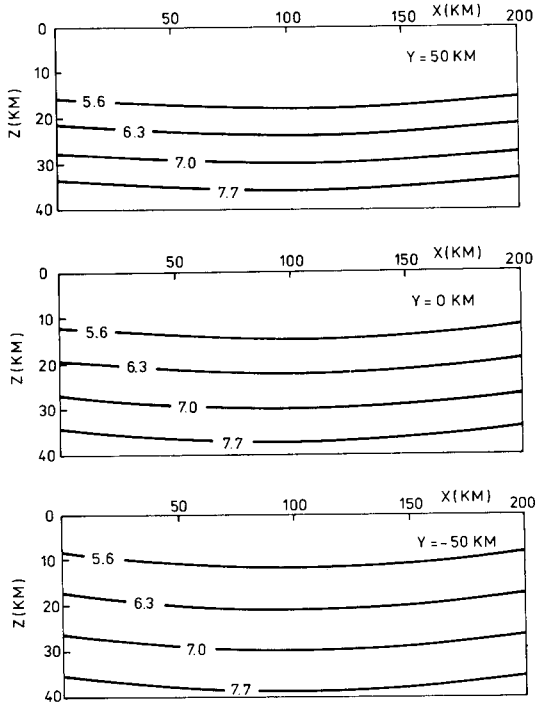

Figure 9. 3-D model used for computing synthetic seismograms shown in Figs 10 and 11. Velocity isolines are shown for three vertical sections corresponding to planes $y = 50$, 0, and -50 km. The point source is situated at $x = y = z = 0$ km.

require a smaller number of rays. The number of rays used in the computation of the seismograms presented in Fig. 8 was only 130; even a smaller number of endpoints of the rays yields practically the same result. The accuracy of the computed synthetic seismograms is approximately the same as for the initial parameters specified at the source, see Fig. 4(b). Again, the results are not very sensitive to the selection of initial parameters.

3.2 COMPUTATION FOR 3-D MODELS

In this section we shall consider a 3-D model in which the velocity varies in all three dimensions. The model is a modification of the model used in Section 3.1. The velocity isolines for three vertical sections, corresponding to planes $y = 50$, 0 and -50 km, are shown in Fig. 9. The reason for choosing this simple model is to demonstrate the possibilities of the described procedures on a 3-D model as simple as possible, which, however, contains some singularity of the ray field.

The point source of *P*-waves is situated at the origin of the Cartesian coordinate system. The synthetic seismograms are computed along three surface straight-line profiles, specified by relations $y = 50$, 0 and -50 km. The receivers are distributed along all the profiles at the following x-coordinate intervals: 95 km $\leqslant x \leqslant$ 155 km.

Fig. 10 shows the termination points of rays used in the computation. The distribution of termination points clearly indicates the influence of lateral velocity variations. The number of termination points along the Earth's surface was 330.

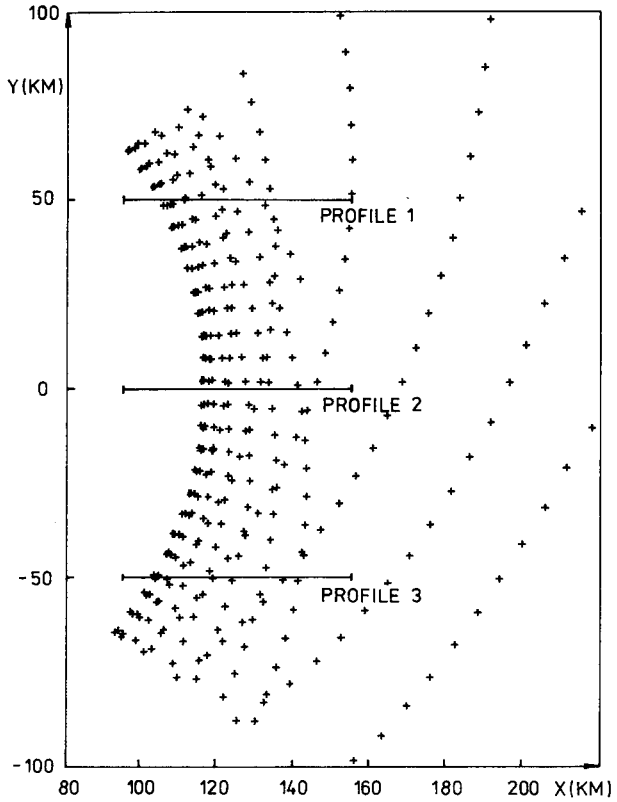

Figure 10. Endpoints of rays at the Earth's surface used for evaluating synthetic seismograms along profiles 1, 2 and 3.

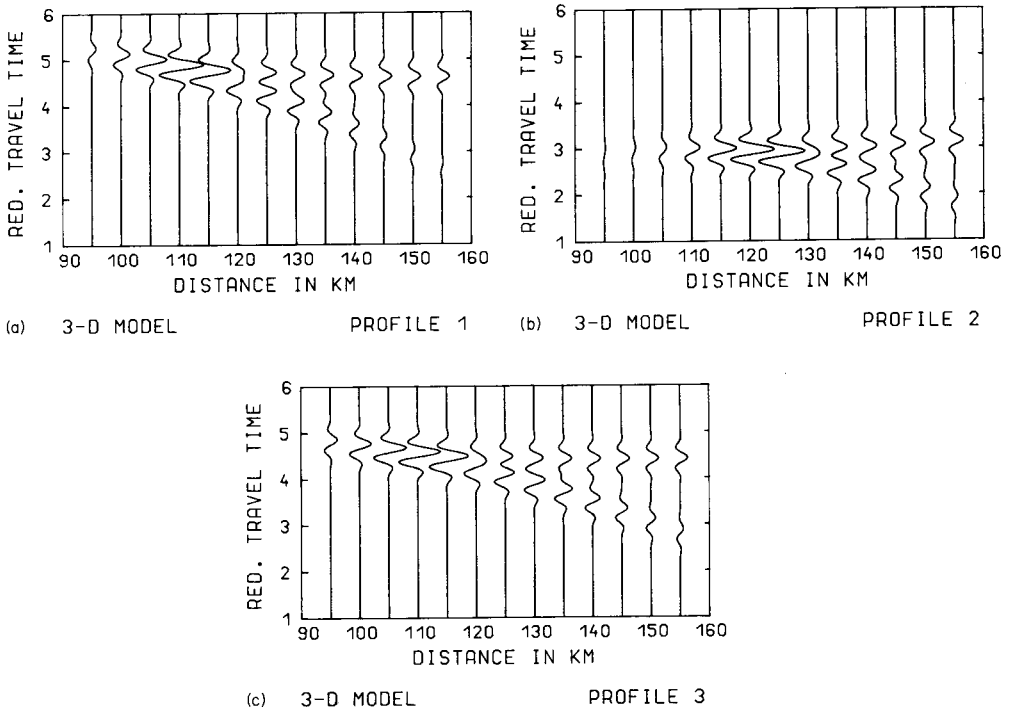

Figure 11. Synthetic seismograms of the vertical displacement vector component of the *P*-refracted wave in the model shown in Fig. 9 along profiles $y = 50, 0$ and -50 km. Prevailing frequency 2 Hz. The travel-time axes are reduced, reduction velocity 6 km s^{-1}. All synthetic seismograms were computed using the Gaussian beam approach with the initial beam parameters specified at the source. The Gaussian beams are stigmatic at the source with $L_0 = 15$ km, $K_0 = 0$ km^{-1}.

Fig. 11 shows the synthetic sections obtained with the Gaussian packet approach along the three profiles for the prevailing frequency of 2 Hz. The synthetic seismograms are again plotted on a reduced time axis; the reduction velocity is 6 km s^{-1}. The reduction was not performed with respect to the epicentral distance, but to the x-coordinate of the receiver. The general character of the synthetic seismograms along all three profiles remains very similar to those described in Section 3.1. Their properties will therefore not be discussed here again.

4 Discussion

In the preceding sections it was shown that the method based on the summation of Gaussian beams can be effectively used to evaluate synthetic body wave seismograms in smooth 3-D laterally varying media. Comparisons with the reflectivity method show that the method yields satisfactorily accurate results even in caustic regions.

The procedure of summation of Gaussian beams can be used even in the case of 'infinitely broad' Gaussian beams, corresponding to paraxial ray approximations. The summation of Gaussian beams of finite widths, however, usually leads to a more satisfactory result with a smaller computing effort than the summation of paraxial ray approximations, as it suppresses the oscillations considerably. Even a slight Gaussian windowing of paraxial ray approximations leads to a considerably higher effectivity of computations, practically without any loss of accuracy of the computations.

The approach based on the summation of Gaussian beams is very flexible because the initial parameters of the Gaussian beams can be chosen in different ways. It includes, as special cases, various modifications of the Chapman–Maslov method, the WKBJ method, the expansion of the point source into plane waves, expansion into paraxial ray approximations, the ray method itself, etc. The results of computation, however, may depend on the choice of the initial parameters of Gaussian beams, particularly if the receiver is situated in a singular region of the ray field (boundary zone between the illuminated and shadow regions, critical region, etc.). The specification of initial parameters of Gaussian beams at the endpoints of rays along the Earth's surface has certain advantages in comparison with the specification of the initial parameters at the source. For example, the size of the effective spots of Gaussian beams can be chosen in accordance with the density of the endpoints of the rays in the neighbourhood of the receiver. Smaller spots can be chosen in regions where the network of the endpoints of the rays is dense and larger spots in regions where the rays are less dense.

It may be possible to determine automatically some 'optimum' initial parameters of Gaussian beams, for which the error of computations would be minimized. In any case, however, it would be very useful to test the accuracy of the Gaussian beam approach by computing seismic wavefields in some other typical structures for which more accurate solutions (obtained by finite differences, integral equations, reflectivity method) are known.

References

Babich, V. M., 1956. Ray method of computing the intensity of wave fronts, *Dokl. Akad. Nauk SSSR,* **110,** 355–357 (in Russian).

Babich, V. M., 1968. Eigenfunctions concentrated in the vicinity of closed geodesics, in *Mathematical Problems of the Theory of Propagation of Waves,* **9,** 15–63, Nauka, Leningrad (in Russian).

Červený, V., 1983. Synthetic body wave seismograms for laterally varying layered structures by the Gaussian beam method, *Geophys. J. R. astr. Soc.,* **73,** 389–426.

Červený, V., Klimeš, L. & Pšenčík, I., 1984. Paraxial ray approximations in the computation of seismic wavefields in inhomogeneous media, *Geophys. J. R. astr. Soc.,* **79,** 89–104.

Červený, V, Molotkov, I. A. & Pšenčík, I., 1977. *Ray Method in Seismology,* Karlova Universita, Praha.

Červený, V., Popov, M. M. & Pšenčík, I., 1982. Computation of wave fields in inhomogeneous media – Gaussian beam approach, *Geophys. J. R. astr. Soc.,* **70,** 109–128.

Červený, V. & Pšenčík, I., 1983. Gaussian beams and paraxial ray approximation in three-dimensional elastic inhomogeneous media, *J. Geophys.,* **53,** 1–15.

Chapman, C. H. & Drummond, R., 1982. Body wave seismograms in inhomogeneous media using Maslov asymptotic theory, *Bull. seism. Soc. Am.,* **72,** 277–317.

Fuchs, K. & Müller, G., 1971. Computation of synthetic seismograms with the reflectivity method and comparison with observations, *Geophys. J. R. astr. Soc.,* **23,** 417–433.

Haines, A. J., 1983. Parabolic approximations for seismic disturbances in laterally varying structures, *PhD thesis,* University of Cambridge.

Karal, F. C. & Keller, J. B., 1959. Elastic wave propagation in inhomogeneous media, *J. acoust. Soc. Am.,* **31,** 694–705.

Kirpichnikova, N. J., 1971. Construction of solutions concentrated close to rays for the equations of elasticity theory in an inhomogeneous isotropic space, in *Mathematical Problems of Theory of Diffraction and Propagation of Waves,* **1,** 103–113, Nauka, Leningrad (in Russian, English translation by American Mathematical Society, 1974).

Klem-Musatov, K. D., 1980. *The Theory of Edge Waves and its Applications in Seismology,* Nauka, Novosibirsk (in Russian).

Klimeš, L., 1984. Expansion of a high-frequency time-harmonic wavefield given on an initial surface into Gaussian beams, *Geophys. J. R. astr. Soc.,* **79,** 105–118.